Mine Water and the Environment (2018) 37:763–773
https://doi.org/10.1007/s10230-018-0537-x

TECHNICAL ARTICLE

# Concurrent Mining During Construction and Water-Filling of a Goaf Groundwater Reservoir in a Coal Mine

**Pan Li[1] · Liqiang Ma[2,3] · Yu Wu[1] · Liqiang Zhang[1] · Yang Hao[1]**

Received: 30 July 2017 / Accepted: 27 March 2018 / Published online: 2 April 2018


**Abstract**
Coal mining has aggravated water scarcity in the arid areas of northwestern China. Concurrent aquifer drainage, mining, and water storage is proposed, using a goaf groundwater reservoir (GGWR) to preserve the area's fragile ecosystem. By continuously draining the overlying aquifer of the working face and simultaneously storing water in the goaf while the working face is mined, this technology can maintain the storage capacity of the GGWR without jeopardizing mine safety. The drainage process was simulated, based on mining conditions of the 11201 working face in the Yuandatan coal mine, to investigate how water pressure variations in the overlying aquifer would affect GGWR construction. Then, two drainage borehole arrangements were simulated. The research demonstrated that the resulting drainage intensity would enable continuous operation of "aquifer drainage-coal mining-water storage", and that the design satisfies the in-situ drainage and storage requirements. Therefore, concurrent construction and water-filling of the GGWR is feasible.

**Keywords** Aquifer drainage · Mine water · Borehole · Mine safety

## Introduction

The ever-increasing demands of water for daily life, irrigation, and industrial production have already consumed water resources and decreased groundwater levels, especially in some coal mining areas, where the loss of water can be severe (Howladar 2013; Kulshreshtha 1998; Qiao et al. 2016; Raju et al. 2013; Zeman et al. 2006). Artificial aquifer recharge has been widely used for years to aid groundwater recovery (Bhattacharya 2010; Brothers and Katzer 1990; Ghanem et al. 2011; Samadder et al. 2011). Natural subsurface aquifers and geological structures have also been used to construct groundwater reservoirs (Deng 2012; Li et al. 2006), and construction of underground reservoirs has greatly promoted artificial groundwater recharge (Deng et al. 2014; Paudyal and Gupta 1987).

China has serious water-scarcity problems, especially in its northwestern arid and semi-arid areas (Miao et al. 2009; Yang et al. 2013), where there are plenty of shallow coal resources (Li et al. 2014). However, coal mining can lead to the loss of water, and even cause water inrush accidents (Mark 2016; Sun et al. 2016; Zhang and Peng 2005; Zhang et al. 2014). In many mining areas, approximately two tons of mine water are discharged to the land surface for every ton of coal mined, which significantly affects the sustainability of coal mining and the ecological balance of those areas (Bian et al. 2009; He et al. 2008; Zhang et al. 2011). However, from the standpoint of recycling, mine water is a reusable resource. In order to avoid wasting water, the mined-out space of coal mines can be used to construct a goaf groundwater reservoir (GGWR) for mine water storage (Andrés et al. 2017; Ma et al. 2009; Ordonez et al. 2012; Sheng 2005).

**Electronic supplementary material** The online version of this article (https://doi.org/10.1007/s10230-018-0537-x) contains supplementary material, which is available to authorized users.

✉ Yu Wu
wuyu@cumt.edu.cn

Liqiang Ma
ckma@cumt.edu.cn

[1] State Key Laboratory for Geomechanics and Deep Underground Engineering, China University of Mining and Technology (CUMT), Xuzhou 221116, Jiangsu, China

[2] School of Mines, CUMT, Xuzhou 221116, Jiangsu, China

[3] Key Laboratory of Deep Coal Resource Mining, Ministry of Education of China, Xuzhou 221116, Jiangsu, China

Consequently, GGWR construction in coal mines has been addressed by some researchers (Chen and Ju 2011; Gu 2013). This technology can be implemented by the following process: first, the coal pillars are connected by artificial dams to form a reservoir dam after anti-seepage treatment; then, mine water entry facilities are constructed for water storage in the goaf, and finally, a water supply system is established, based on mine water purification. A GGWR differs from more conventional underground reservoirs in three ways:

1. Goafs can provide large amounts of water storage space. In the arid and semi-arid mining areas of China, the main coal seams are large and thick. For instance, the mining height, layout length, and advancing length of the working face in the Shendong mining area can reach 5, 300, and 5000 m, respectively (Gao and He 2010).
2. The GGWR has high hydraulic conductivity, which aids water extraction. There are plenty of interstices between the collapsed rocks in the goaf and, in addition, large numbers of fractures form in the rock mass above the rubble.
3. Conventional mining generates a great deal of mine water, which can be the water source for a GGWR (Li and Zhou 2006; Zhang and Shen 2004). Restricting the mining height and backfilling can protect the overlying aquifers, but will cause coal loss and affect a mine's productivity (Cao et al. 2014). Figure 1 shows the schematic diagram of GGWR construction under different mining conditions.

However, the safety of coal pillar dams and safe storage capacity limits had not been well studied. Therefore, researchers studied the stress and stability of coal pillar dams during earthquakes, and developed a safety factor for coal pillar dams (Gu et al. 2016a). In addition, dam design and GGWR storage capacity were researched (Chen et al. 2016). Through theoretical analysis and in-situ measurements, the safe maximum storage capacity of a GGWR was studied as well (Ju et al. 2017). By the end of 2015, 35 GGWRs with about $31 \times 10^6$ $m^3$ of total storage capacity had been constructed in the Shendong mining area. These GGWRs have supplied approximately $60 \times 10^6$ $m^3$ of water and brought economic benefits of more than $3 \times 10^9$ ¥ ($0.45 \times 10^9$ US$)

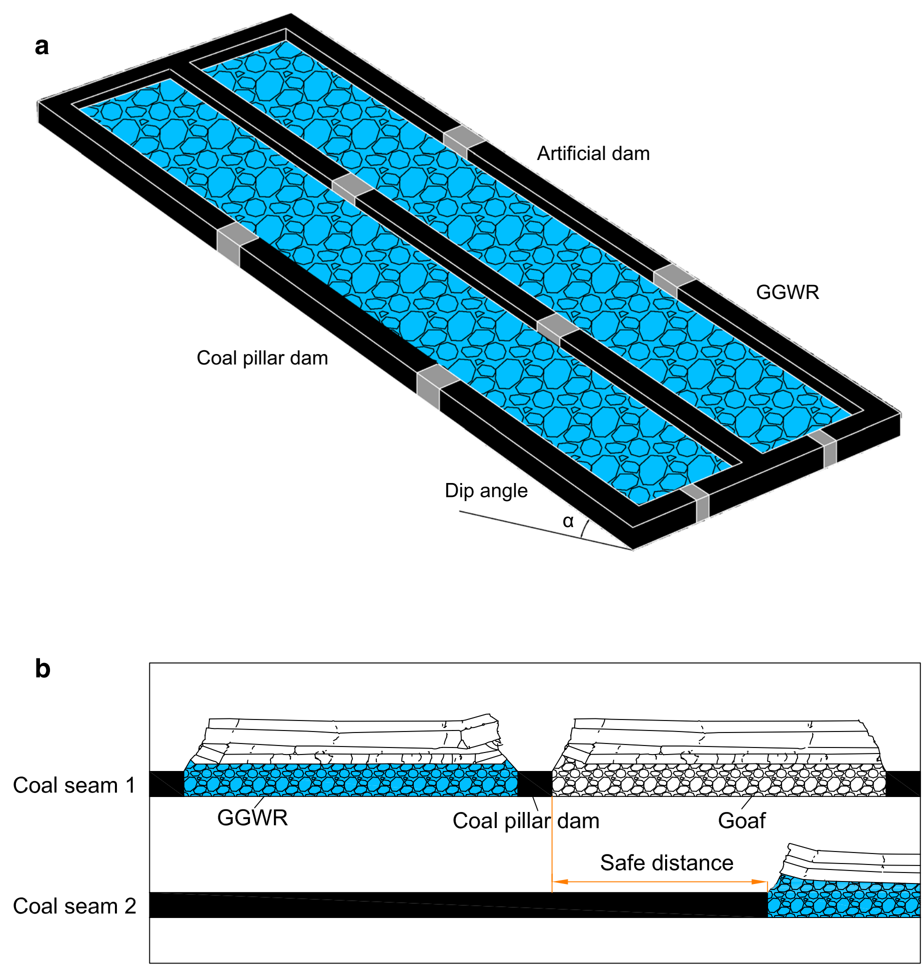


**Fig. 1** Schematic diagram of GGWR construction in the coal mine (**a** single coal seam mining, **b** coal seam group mining)

for the Shendong area. This approach has been proposed for the Xinjie and Wuhai mining areas and the Tarangaole mine (Gu et al. 2016b).

Mining can cause water in overlying aquifers and surface water to flow into the mine, and flow of water into unreconstructed goafs is generally hard to control and manage (Dong 2016; Wu et al. 2013). But with current GGWRs, the process of transferring and then storing mine water in the goaf (after mining of the working face is completed) results in mine water loss, and because the space between the collapsed rock of the goaf is compacted by the overlying strata, the water storage space is reduced.

In this study, the concurrent operation of "aquifer drainage-coal mining-water storage" for construction and water-filling of a GGWR was proposed for the 11201 working face of the Yuandatan coal mine. The drainage of the overlying aquifer using two types of drain intensity was simulated, and based on the results, the drainage borehole design was applied to the GGWR construction there.

## Concurrent Operation Technology

### Concurrent Operation of "Aquifer Drainage-Coal Mining-Water Storage"

Water-rich aquifers above the coal seam are drained by advance drainage boreholes, which are generally drilled upwards from the roadways of the working face when the first weighting of the main roof occurs, to continuously drain the overlying aquifer as the working face advances. The water is simultaneously stored in the goaf. Figure 2 outlines the construction and water-filling process.

The first and second working faces (A and B) are placed, and the anti-seepage treatment is applied to the coal pillars of the working faces (Fig. 3a). During the initial mining period (working face A), water conductive fractures slowly

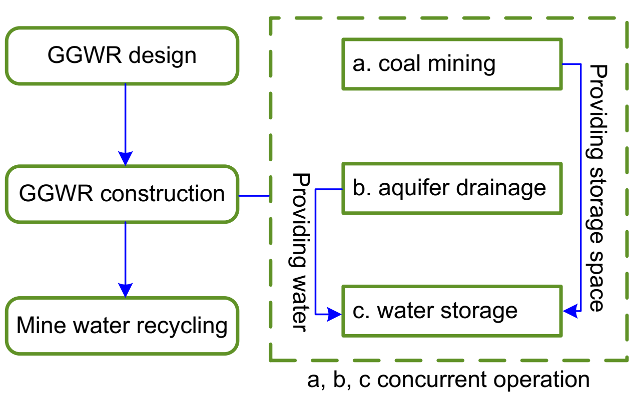


**Fig. 2** GGWR construction through the concurrent operation of "aquifer drainage-coal mining-water storage"

develop in the strata overlying the goaf, and the water of the overlying aquifer is drained by boreholes in two roadways of working face A and the air-return roadway (working face B; see Fig. 3b). Using retreating mining, the mine water (aquifer drainage and water for the equipment) can be efficiently stored in the goaf of working face A. When working face A has advanced to a location close to the roadway connected to the coal pillar, the connection roadway is sealed to form an artificial dam with a controllable drainage channel at its bottom. Mine water from working face B is drained to the goaf of working face A through the drainage channels. Drainage intensity is enhanced when water-conductive fractures in the strata overlying the goaf are connected to the aquifer. As mining is completed at working face A, channels between it and the main roadways of the area are sealed and a GGWR is formed (Fig. 3c, d). Working face B is then exploited, while the next working face is prepared and aquifer drainage starts.

After the auxiliary water purifier and booster pump are installed, GGWRs can provide water for the land surface and mine production through the water supply system. Moreover, when more than one seam is being mined, water in the upper seam's GGWR can be used for power generation through water transfer between the coal seams (Xie et al. 2015).

### Design Method of Drainage Borehole

According to the factors that influence aquifer drainage, which mainly consist of water pressure, aquifer permeability, and mining impact, the drainage intensity of the borehole can be divided into three grades: high (I), medium (II), and low intensity (III). Figure 4 illustrates the design process. The borehole arrangements, which include the number, angle, diameter, and drilling depth of boreholes are determined by the drainage intensity requirements.

### Construction of the Water Storage Space

1. A region with steady strata, a small dip angle of the coal seam (8° or less), and simple geology is the optimal site for layout of the first working face. For multiple seam mining, mine water from the first main coal seam can be released through drainage channels and stored in the goaf of the next lower main coal seam, as long as there is enough distance between the two seams to be safe. After anti-seepage treatment, about 25 m wide coal pillars remain to form the GGWR dams (Gu 2015).
2. As the working face is mined, the caving and fractured zones in the strata overlying the goaf can provide water storage space (Jardon et al. 2013). The volume of water storage space is calculated as Eq. (1):

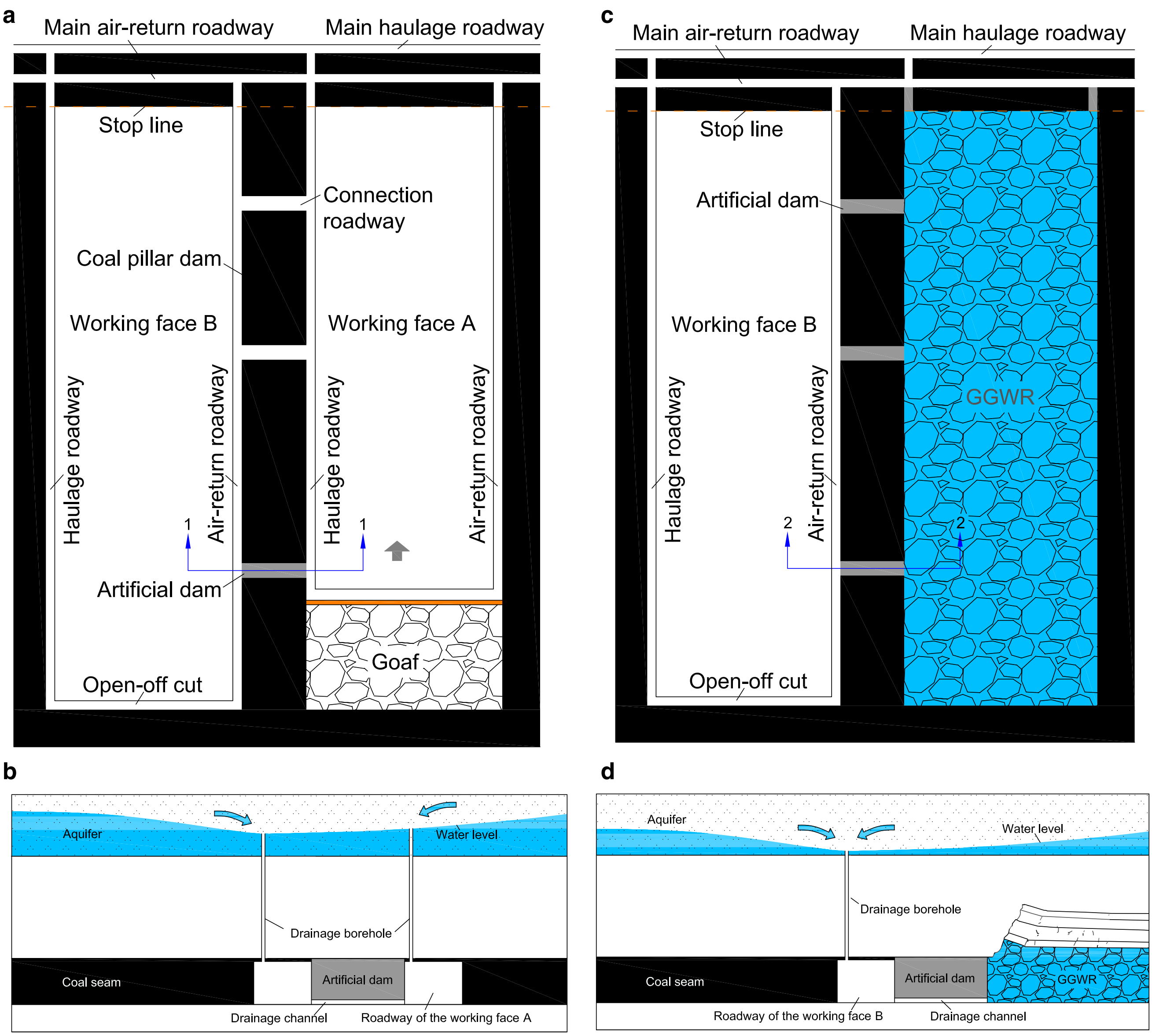


**Fig. 3** Process of the GGWR construction (**a** layout of the mining working face, **b** 1–1 profile of drainage boreholes layout, **c** diagram of water storing, **d** 2–2 profile of GGWR)

$$V = KSM\left(1 - \frac{W_{\max}}{M\cos\alpha}\right) \quad (1)$$

where: $V$ is the volume of the water storage space (in $m^3$), $K$ is the coefficient of water storage capacity (ranging from 15 to 25%), $S$ is the area of the goaf (in $m^2$), $M$ is the mining height of coal seam (in m), $W_{max}$ is the maximum amount of surface subsidence (in m), and $\alpha$ is the dip angle of the coal seam (in degrees).

3. The first temporary water retaining wall is constructed behind the hydraulic supports when the working face is advanced to the first weighting of the main roof, and then the water is stored in the goaf to form the initial secondary reservoir (Fig. 5a). Subsequently, the second temporary water retaining wall is constructed before the working face is advanced to the first periodic weighting of the main roof, while the first temporary water retaining wall is destroyed after the first periodic weighting of the main roof. As a consequence, the two secondary reservoirs are connected to form a new secondary reservoir (Fig. 5b). With the advancing of working face, the above process is repeated constantly until a complete GGWR is formed.

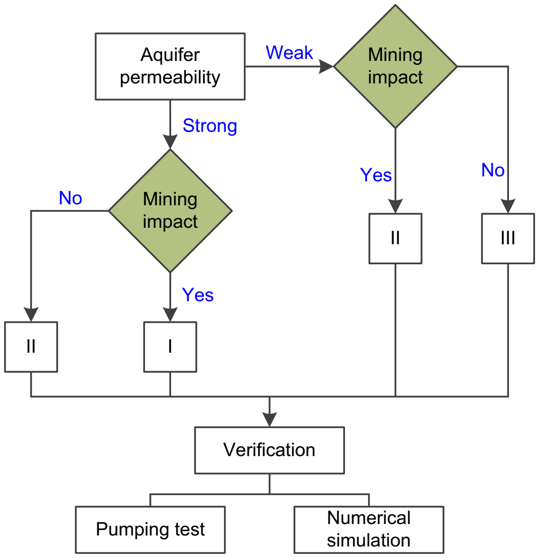


**Fig. 4** Design process of the drainage boreholes

4. The temporary water retaining wall, with a width of 20 cm and a height of 1.7 m, is a low strength rigid material. Additionally, drainage and pumping pipes surrounded by protective material are laid at the bottom corner of the connection between the coal pillar dam and the temporary water retaining wall (Fig. 6).

## Design of the GGWR in the Yuandatan Coal Mine

### Mining and Hydrological Characteristics of the Yuandatan Mine

Coal seam 2 of the Yuandatan coal mine in the Yuheng mining area is 180.71–420.93 m below the surface and 1.21–4.12 m thick. The Yuheng mining area has an arid and semi-arid temperate continental monsoon climate, with an annual average precipitation of 316–513 mm, making it the lowest rainfall area in Shaanxi province. About two-thirds of the annual precipitation is concentrated in July–September.

The Yuandatan coal mine is located at the junction of three aquifer systems: a Cretaceous clastic rock fracture aquifer system, a Carboniferous–Jurassic clastic rock fractured aquifer system, and a Quaternary overlying loose layer

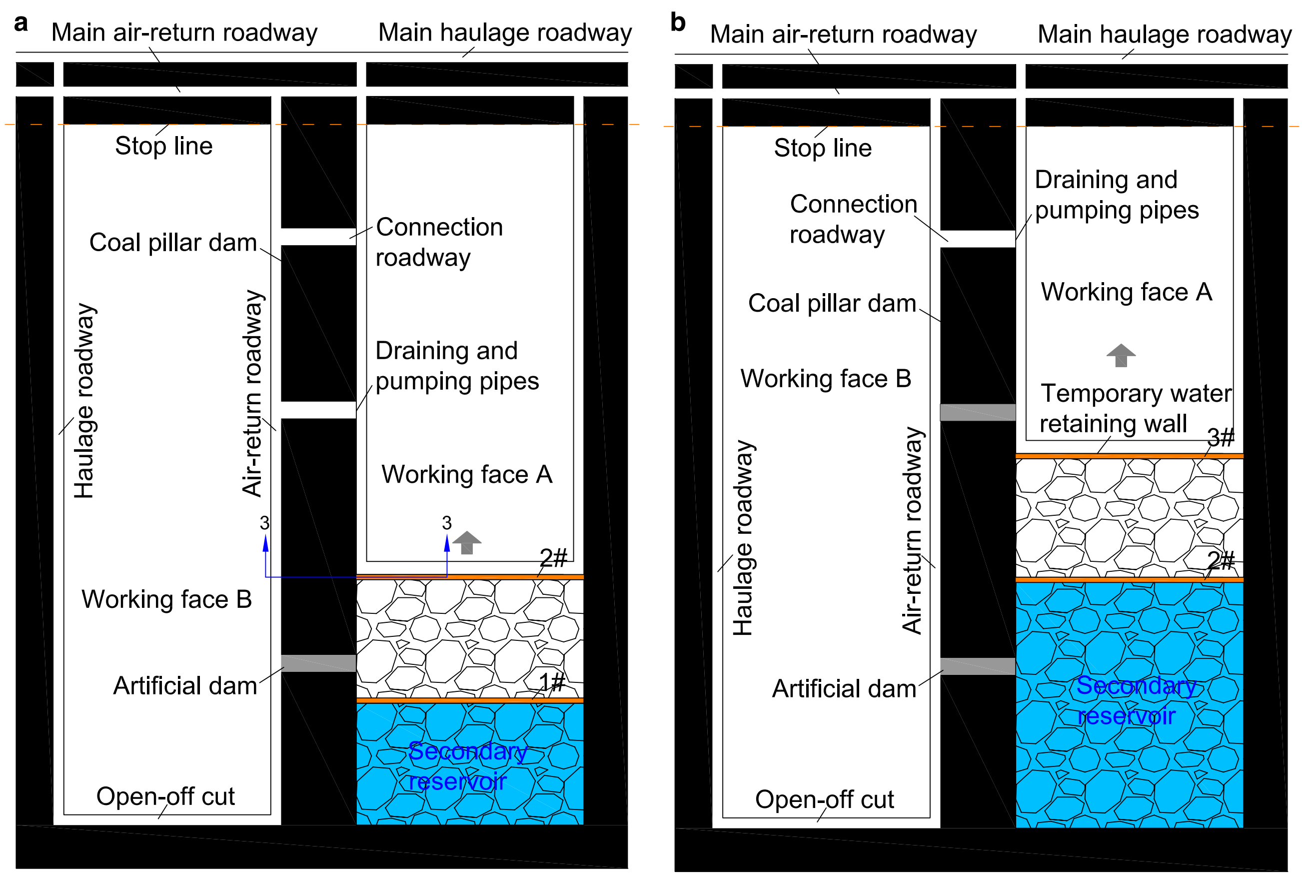


**Fig. 5** Formation process of the secondary reservoir (**a** initial secondary reservoir, **b** new secondary reservoir)

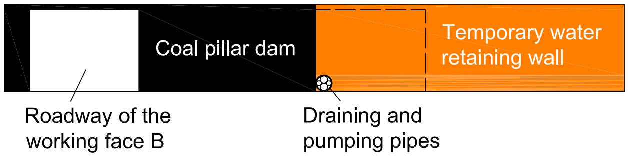


**Fig. 6** Design of the temporary water retaining wall (3–3 profile)

pore aquifer system. The aquifers of the Yuandatan mine field are divided into three aquifer zones and two aquifuge zones from top to bottom (Table 1). In the study area, the aquifer above coal seam 2 is the Jurassic (Zhiluo Group) confined aquifer (the 2nd aquifer zone), while the aquifuge is the section from the top of the Jurassic Yan'an Group to the silty sandstone roof of the coal seam 2 (the 2nd aquifuge zone).

## Continuous Drainage Design of Overlying Aquifer

The drainage of the aquifer overlying the 11201 working face was simulated through COMSOL Multiphysics, based on the conditions of the confined aquifer above coal seam 2. Given the width of the two working faces, the simulation domain was a 660 × 32 m rectangle, according to the thickness of the aquifer and the width of the coal pillar. Based on the range of influence of the water-conductive fractures to the aquifer, one of two borehole arrangements was simulated. The first type (Fig. 7a) represented the layout of drainage boreholes before the aquifer is damaged by mining. One vertical drainage borehole with a diameter of 113 mm and a length of 15 m was placed in each of the two 11201 working face roadways and one was placed in the air-return roadway of the 11202 working face. The second type represented the layout of the drainage boreholes after the aquifer is damaged by mining (Fig. 7b).

**Table 1** Aquifers division in Yuandatan mine field

| Stratum era | | | Thickness (m), min–max | Aquifers division | Lithology |
|---|---|---|---|---|---|
| System | Division | Group | | | |
| Quaternary | Holocene ($Q_4$) | $Q_4^{eol}$ | 41.00–145.63 | 1st aquifer zone | Aeolian sand |
| | Upper Pleistocene ($Q_3$) | Salawusu ($Q_{3s}$) | | | Silty clay |
| | Mid Pleistocene ($Q_2$) | Lishi ($Q_{2l}$) | | | Sandy clay |
| Cretaceous | Lower ($K_1$) | Luohe ($K_{1l}$) | | | Coarse sandstone |
| Jurassic | Mid ($J_2$) | Anding ($J_{2a}$) | 57.50–147.19 | 1st aquifuge zone | Mudstone and fine sandstone |
| | | Zhiluo ($J_{2z}$) | 77.70–195.74 | 2nd aquifer zone | Medium coarse sandstone |
| | | Yan'an ($J_{2y}$) | 0–38.05 | 2nd aquifuge zone | Silty mudstone |
| | | | 19.98–60.43 | 3rd aquifer zone | Coarse feldspathic sandstone |

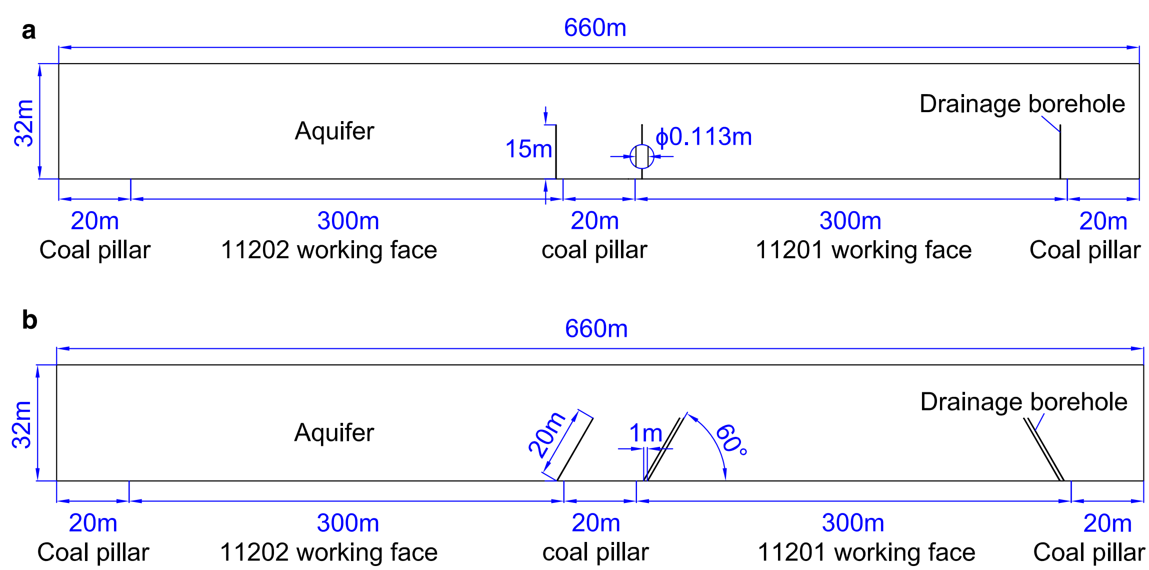


**Fig. 7** Layout of the drainage boreholes for overlying aquifer drainage (**a** before the aquifer is damaged by mining, **b** after the aquifer is damaged by mining)

With a diameter of 113 mm and a length of 20 m, two inclined drainage boreholes were placed in each of the two 11201 working face roadways and one was placed in the air-return roadway of the 11202 working face.

The models mainly dealt with the process of fluid flow in the aquifer under the action of overburden pressure. The mass conservation and momentum conservation of water flow in the aquifer can be described by the following equations (Wu 2012):

$$\frac{\partial(\rho n)}{\partial t} + \nabla \bullet (\rho \boldsymbol{u}) = 0 \tag{2}$$

$$\frac{\partial(\rho \boldsymbol{u})}{\partial t} + \frac{\rho \boldsymbol{u}}{n} \bullet \nabla \boldsymbol{u} = -\nabla P + \nabla \bullet (\mu \nabla \boldsymbol{u}) - \frac{\mu}{k}\boldsymbol{u} + n\rho \boldsymbol{g} = 0 \tag{3}$$

where $\rho$, $\boldsymbol{u}$, and $\mu$ are the density, velocity vector, and viscosity of water, respectively. $k$, $n$, $\boldsymbol{g}$, $P$ denote the permeability, porosity of the aquifer, gravitational acceleration, and pressure, respectively. Since the water is assumed to be incompressible, $\rho$ is constant. Taking into account the constant load effect of the overlying strata on the aquifer, the porosity ($n$) of aquifer can be expressed as Eq. (4) (Wu 2009):

$$n = 1 - (1 - n_0)e^{(-\beta(p-p_0))} \tag{4}$$

where $p$ is the seepage pressure of water, $\beta$ is the compression coefficient of a moderately porous skeleton, and $n_0$ and $p_0$ are initial porosity and initial seepage pressure, respectively. Three boundaries of each drainage borehole in the models were water flow boundaries and others were no flow boundaries (Supplemental Fig. 1). The initial water pressure of the aquifer was 1.0 MPa, and the pressure at each water flow boundary was 1 atm.

Corresponding parameters of the models are given in Supplemental Table 1. A horizontal measuring line was arranged at the middle of the aquifer (Fig. 8). The water pressure distribution of the aquifer, after 1, 3, 7, and 11 days of drainage were plotted in Supplemental Fig. 2 and Fig. 3, where the former represents the stage before the aquifer damage, while the latter represents the stage after the damage. The water pressure variation of the measuring line for these two stages were represented in Figs. 9 and 10.

In each drainage roadway, the next group of boreholes were placed after the 11201 working face reaches the former group of drainage boreholes; the distance between the two groups of drainage boreholes is 100 m. After 11 days of drainage, the maximum water pressure in the aquifer above the middle of the 11201 working face decreased to 0.8 MPa for the first type borehole arrangement and 0.5 MPa for the second type, respectively. Since the average advancing speed of the 11201 working face is 7 m per day, the water pressure of aquifer is greatly reduced when the working face is advanced from the former group of drainage boreholes to the next group (about 14 days for 100 m), and water inrush will be avoided at the 11201 working face.

## Storage Space Design of the Goaf

The 11201 working face has a layout length of 300 m, an advancing length of 4300 m, and an average mining height of 2.2 m. The width of the coal pillar dam is 20 m, the average dip angle of the coal seam is 6°, and the amount of surface subsidence is 0.6 m. According to Eq. (1), the

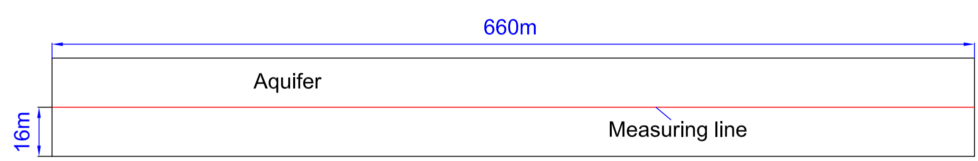


**Fig. 8** Layout of the horizontal measuring line

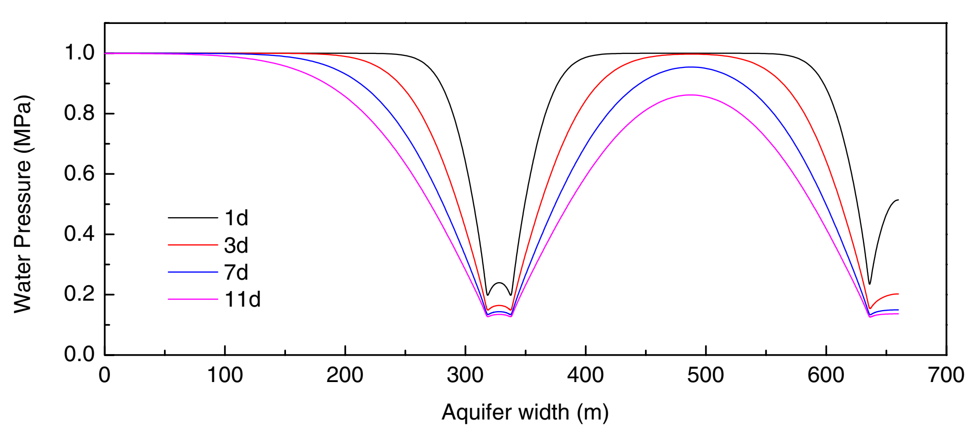


**Fig. 9** Water pressure variation with drainage time at the measuring line before the damage of the aquifer

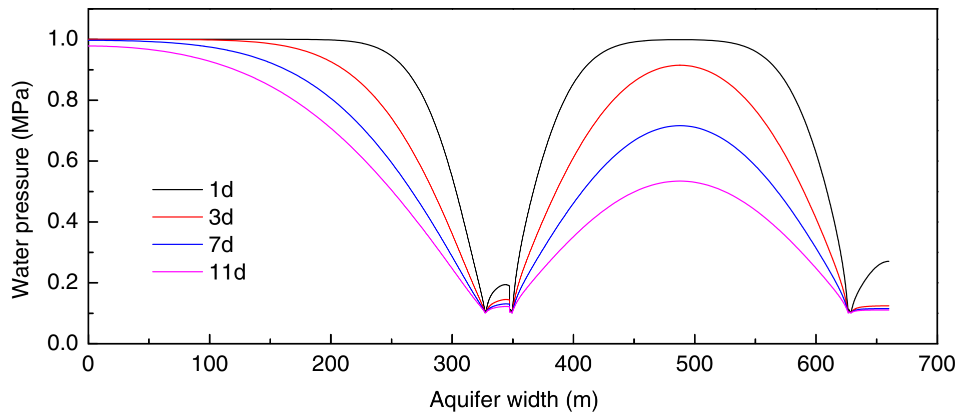


**Fig. 10** Water pressure variation with drainage time at the measuring line after the damage of the aquifer

GGWR design storage space of the 11201 working face is 0.309–0.515 million $m^3$.

## Project Practice of GGWR

### Drainage of the Overlying Aquifer

The pore-fracture confined aquifer of the 2nd aquifer zone will be revealed as the 11201 working face is mined. From the perspective of water control, the aquifer was divided into two sections and two pumping tests were conducted to analyze the effect of the drainage. The borehole layout is shown in Fig. 11.

First, boreholes ZLC-2 and ZLC-6 were used to drain water from the lower section aquifer of the Zhiluo Group, while the water levels in that aquifer was observed in boreholes ZLG-1, ZLG-2, ZLG-5, and ZLG-6, and the water level in the upper section aquifer was observed in boreholes ZLC-1 and ZLC-5. Then, pump tests of the upper and lower section aquifers were conducted using boreholes ZLC-1, ZLC-2, ZLC-5, and ZLC-6.

The first pumping test results are shown in Table 2. After the water levels of the lower section pumping boreholes ZLC-2 and ZLC-6 stabilized at drawdowns of 47.19 and 43.06 m, respectively; the drawdowns of the upper section observation boreholes ZLC-1 and ZLC-5 were 0 and 6.04 m, respectively, while the drawdowns of the lower section observation boreholes ZLG-2 and ZLG-6 were 11.11 and 13.37 m, respectively. Hence, the upper and lower section aquifers are hydraulically connected. Even though the height of the water-conductive fracture had not reached the upper section aquifer, water from it will slowly seep into the mine.

The results of the second pumping test indicate that the Zhiluo Group aquifer water is easily drained (Table 3). The borehole bottom location of the drainage borehole should be arranged in the medium sandstone of the Zhiluo Group's lower section.

### Water Storage Effect

Currently, the 11201 working face has advanced to 850 m. The water level of the GGWR is 0.6 m and the volume of water storage is about 30,600 $m^3$. The design storage capacity of this part of the GGWR is 84,100 $m^3$; the actual storage volume is 36% of the design capacity. Therefore, as the 11201 working face advances, the water from the overlying aquifer and the land surface, which is connected through the water-conductive fractures, will be safely stored in the GGWR.

## Discussion

The water-conductive fractures in the overlying strata of the goaf will experience three stages: initial development, rapid development, and compaction closure; water inrush can be avoided by decreasing the water pressure of the aquifer before the second stage. In this study, the effect of the location and broken form of the key strata on the development of and the height of the water-conductive fractures was not considered. This is mainly because the drainage intensity of the boreholes will be adjusted for different key strata conditions.

In addition, the aquifer in the models was assumed to be a homogeneous, isotropic, porous medium and the drainage of the aquifer, saturated seepage. However, water-conductive fractures induced by mining may develop to the upper aquifers or to the surface, which will affect unsaturated seepage and make the flow behaviors much more complicated to study (Wu et al. 2007), since the surface water will flow through the soil and rock layers, and then into the GGWR. Because of the heterogeneity between the fractured strata, the difference in hydraulic conductivity will induce capillary barrier effects, which could block the downward seepage of the surface water under certain conditions (Wu et al. 2002). This effect is beneficial for nuclear waste storage, but not for GGWR construction, since the surface water formed

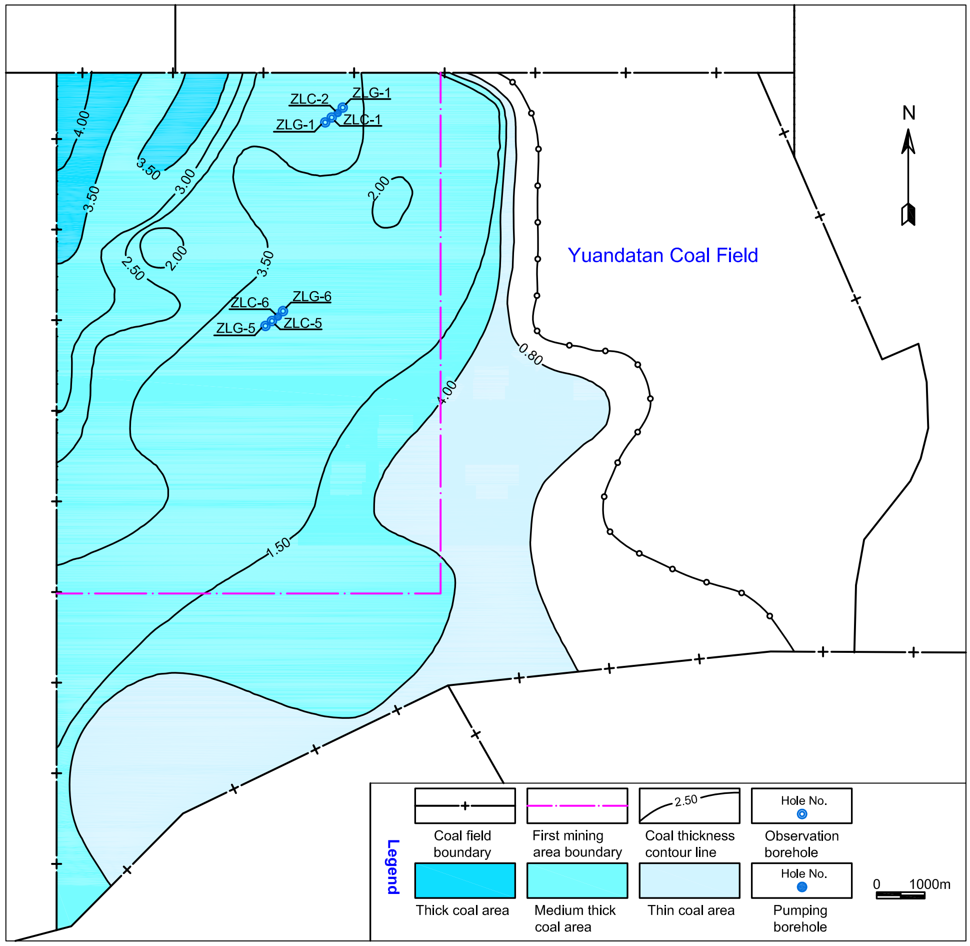


**Fig. 11** Layout of the drainage boreholes for pumping test

**Table 2** Water level change of upper and lower section of Zhiluo Group when pumping lower section

| Main pumping borehole | | | | Observation borehole | | | |
|---|---|---|---|---|---|---|---|
| Hole no. | Pumping position | Initial water level (m) | Drawdown (m) | Hole No | Observation position | Initial water level (m) | Drawdown (m) |
| ZLC-2 | Lower $J_{2z}$ | 62.41 | 47.19 | ZLG-1 | Lower $J_{2z}$ | 63.45 | 7.91 |
| | | | | ZLG-2 | Lower $J_{2z}$ | 63.70 | 11.11 |
| | | | | ZLC-1 | Upper $J_{2z}$ | 14.24 | 0 |
| ZLC-6 | Lower $J_{2z}$ | 43.17 | 43.06 | ZLG-5 | Lower $J_{2z}$ | 46.28 | 8.13 |
| | | | | ZLG-6 | Lower $J_{2z}$ | 43.60 | 13.37 |
| | | | | ZLC-5 | Upper $J_{2z}$ | 31.45 | 6.04 |

**Table 3** Pumping test results of drainage difficulty verification for Zhiluo Group aquifer

| Hole no. | Pumping position | Drawdown, S (m) | Water yield, Q ($m^3$/min) | S/Q | Verification result |
|---|---|---|---|---|---|
| ZLC-1 | Upper $J_{2z}$ | 20.90 | 0.0289 | 722.68 > 10 | Easy to drain |
| ZLC-5 | Upper $J_{2z}$ | 17.90 | 0.0324 | 552.47 > 10 | Easy to drain |
| ZLC-2 | Lower $J_{2z}$ | 7.91 | 0.0450 | 175.78 > 10 | Easy to drain |
| ZLC-6 | Lower $J_{2z}$ | 8.13 | 0.0209 | 388.25 > 10 | Easy to drain |

by rainfall cannot rapidly flow into the GGWR. However, surface storage will lead to large evaporative losses, which is not conducive to water resource protection. The seepage characteristics of the water in the fractured rock near the GGWR will be further studied.

## Conclusions

In this paper, we suggest concurrent "aquifer drainage-coal mining-water storage" for construction and water-filling of a GGWR for the 11201 working face of the Yuandatan coal mine. The main conclusions of this research are:

1. Three vertical boreholes and five inclined boreholes were used respectively to drain the overlying aquifer of the 11201 working face before and after the aquifer was damaged by mining, to ensure the continuity of the concurrent "aquifer drainage-coal mining-water storage" operation, as well as safe mining.
2. The storage volume should reach 36% of the design storage capacity of this part of the GGWR after the 11201 working face is advanced to 850 m. As the working face advances, the aquifer water of the Zhiluo Group's upper section and surface water may seep into the goaf, which will increase the GGWR's water storage volume. Concurrent operation of "aquifer drainage-coal mining-water storage" for construction and water-filling of the GGWR appears to be feasible.

**Acknowledgements** This work was financed by the National Natural Science Foundation of China with grant 51674247. The authors furthermore thank the anonymous reviewers and related editors who have significantly enhanced the quality of this paper.

## References

Andrés C, Ordóñez A, Álvarez R (2017) Hydraulic and thermal modelling of an underground mining reservoir. Mine Water Environ 36:24–33

Bhattacharya AK (2010) Artificial ground water recharge with a special reference to India. Int J Res Rev Appl Sci 4:214–221

Bian ZF, Lei SG, Inyang HI, Chang LQ, Zhang RC, Zhou CJ, He X (2009) Integrated method of RS and GPR for monitoring the changes in the soil moisture and groundwater environment due to underground coal mining. Environ Geol 57:131–142

Brothers K, Katzer T (1990) Water banking through artificial recharge, Las Vegas Valley, Clark County, Nevada. J Hydrol 115:77–103

Cao ZG, He RM, Wang XF (2014) Coal mining affected to underground water and underground water storage and utilization technology. Coal Sci Technol 42:113–116, 128 **(Chinese)**

Chen SS, Ju JF (2011) Utilization technology of mine water resources in Daliuta mine. Coal Sci Technol 39:125–128 **(Chinese)**

Chen SS, Huang QX, Xue G, Li RQ (2016) Technology of underground reservoir construction and water resource utilization in Daliuta coal mine. Coal Sci Technol 44:21–28 **(Chinese)**

Deng MJ (2012) Ground reservoir: a new pattern of groundwater utilization in arid north-west China—a case study in Tailan river basin. Proced Environ Sci 13:2210–2221

Deng MJ, Li WP, Li T, Shu LC (2014) Investigation of key technologies for underground water storage structures and groundwater reservoirs in Xinjiang. Quat Sci 34:918–932 **(Chinese)**

Dong SN (2016) Assessment of coal mining impact on water resources. In: Hawkins E (ed) Study on the optimal allocation of water resources systems and the comprehensive utilization of water resources in arid-semiarid multiple mining areas. Springer, Cham, pp 149–169

Gao JE, He HT (2010) Application of fully mechanized full seam one passing mining technology to thick seam in Shendong mining area. J Chin Coal Soc 35:1888–1892 **(Chinese)**

Ghanem M, Marei A, Hoetzl H, Wolf L, Ali W, Assi A (2011) Assessment of artificial recharge test in Jeftlik Faria area, West Bank. J Water Resour Protect 03:186–191

Gu DZ (2013) Water resource and surface ecology protection technology of modern coal mining in China's energy "Golden Triangle". Eng Sci 15:102–107 **(Chinese)**

Gu DZ (2015) Theory framework and technological system of coal mine underground reservoir. J Chin Coal Soc 40:239–246 **(Chinese)**

Gu DZ, Yan YG, Zhang Y, Wang EZ, Cao ZG (2016a) Experimental study and numerical simulation for dynamic response of coal pillars in coal mine underground reservoir. J Chin Coal Soc 41:1589–1597 **(Chinese)**

Gu DZ, Zhang Y, Cao ZG (2016b) Technical progress of water resource protection and utilization by coal mining in China. Coal Sci Technol 44:1–7 **(Chinese)**

He XW, Yang J, Shao LN, LI FQ, Wang XC (2008) Problem and countermeasure of mine water resource regeneration in China. J Chin Coal Soc 33:63–66 **(Chinese)**

Howladar MF (2013) Coal mining impacts on water environs around the Barapukuria coal mining area, Dinajpur, Bangladesh. Environ Earth Sci 70:215–226

Jardon S, Ordonez A, Alvarez R, Cienfuegos P, Loredo J (2013) Mine water for energy and water supply in the Central Coal Basin of Asturias (Spain). Mine Water Environ 32:139–151

Ju JF, Xu JL, Zhu WB (2017) Storage capacity of underground reservoir in the Chinese western water-short coalfield. J Chin Coal Soc 42:381–387 **(Chinese)**

Kulshreshtha SN (1998) A global outlook for water resources to the year 2025. Water Resour Manag 12:167–184

Li GY, Zhou WF (2006) Impact of karst water on coal mining in North China. Environ Geol 49:449–457

Li WL, Shu LC, Yin ZZ (2006) Concept and design theory of groundwater reservoir. J Hydraul Eng 37:613–618 **(Chinese)**

Li WP, Li T, Chen W, Chang JY, Wang QQ (2014) Goaf water storage—a new way for water preserved mining in arid areas. J Eng Geol 22:1003–1007 **(Chinese)**

Ma LQ, Zhang DS, Li X, Fan GW, Zhao YF (2009) Technology of groundwater reservoir construction in goafs of shallow coalfields. Min Sci Technol 19:730–735

Mark C (2016) Science of empirical design in mining ground control. Int J Min Sci Technol 26:461–470

Miao XX, Wang A, Sun YJ, Wang LG, Pu H (2009) Research on basic theory of mining with water resources protection and its application to arid and semi-arid mining areas. Chinese J Rock Mech Eng 28:217–227 **(Chinese)**

Ordonez A, Jardon S, Alvarez R, Andres C, Pendas F (2012) Hydrogeological definition and applicability of abandoned coal mines as water reservoirs. J Environ Monit 14:2127–2136

Paudyal GN, Gupta AD (1987) Operation of a groundwater reservoir in conjunction with surface water. Int J Water Resour Dev 3:31–43

Qiao W, Li WP, Li T, Chang JY, Wang QQ (2016) Effects of coal mining on shallow water resources in semiarid regions: a case study in the Shennan mining area, Shaanxi, China. Mine Water Environ 36:104–113

Raju NJ, Reddy TVK, Muniratnam P, Gossel W, Wycisk P (2013) Managed aquifer recharge (MAR) by the construction of subsurface dams in the semi-arid regions: a case study of the Kalangi river basin, Andhra Pradesh. J Geol Soc India 82:657–665

Samadder RK, Kumar S, Gupta RP (2011) Paleochannels and their potential for artificial groundwater recharge in the western Ganga plains. J Hydrol 400:154–164

Sheng ZP (2005) An aquifer storage and recovery system with reclaimed wastewater to preserve native groundwater resources in El Paso, Texas. J Environ Manag 75:367–377

Sun WJ, Zhou WF, Jiao J (2016) Hydrogeological classification and water inrush accidents in China's coal mines. Mine Water Environ 35:214–220

Wu YQ (2009) Geohydraulics. Science Press Co. Ltd, Beijing **(Chinese)**

Wu YQ (2012) Mathematical method of flow and contaminant transport in porous media. Science Press Co. Ltd, Beijing **(Chinese)**

Wu YS, Zhang W, Pan LH, Hinds J, Bodvarsson GS (2002) Modeling capillary barriers in unsaturated fractured rock. Water Resour Res 38:35-1–35-12

Wu YS, Lu GP, Zhang K, Pan LH, Bodvarsson GS (2007) Analyzing unsaturated flow patterns in fractured rock using an integrated modeling approach. Hydrogeol J 15:553–572

Wu Q, Cui FB, Zhao SQ, Liu SQ, Zeng YF, Gu YW (2013) Type classification and main characteristics of mine water disasters. J Chin Coal Soc 38:561–565 **(Chinese)**

Xie HP, Hou ZM, Gao F, Zhou L, Gao YN (2015) A new technology of pumped-storage power in underground coal mine: principles, present situation and future. J Chin Coal Soc 40:965–972 **(Chinese)**

Yang H, Flower RJ, Thompson JR (2013) Sustaining China's water resources. Science 339:141–141

Zeman C, Rich M, Rose J (2006) World water resources: trends, challenges, and solutions. Rev Environ Sci Bio 5:333–346

Zhang JC, Peng SP (2005) Water inrush and environmental impact of shallow seam mining. Environ Geol 48:1068–1076

Zhang JC, Shen BH (2004) Coal mining under aquifers in China: a case study. Int J Rock Mech Min 41:629–639

Zhang DS, Fan GW, Ma LQ, Wang XF (2011) Aquifer protection during longwall mining of shallow coal seams: a case study in the Shendong coalfield of China. Int J Coal Geol 86:190–196

Zhang JX, Jiang HQ, Deng XJ, Ju F (2014) Prediction of the height of the water-conducting zone above the mined panel in solid backfill mining. Mine Water Environ 33:317–326